ON INVESTIGATING INSTANTANEOUS WIND-DRIVEN INFILTRATION RATES USING CO_2 DECAY METHOD

Dimitrios Kraniotis*, Tormod Aurlien, Thomas K. Thiis

Department of Mathematical Sciences and Technology, Norwegian University of Life Sciences
Drøbakveien 31, P.O. box: 5003, IMT, N-1423, Ås, Norway
**Corresponding author: dimitrios.kraniotis@umb.no*

ABSTRACT

Carbon dioxide has been already recognized as a potential tracer gas towards estimation of the mean air exchange rates (ACH) of a room or building. The wind direction and mean wind velocity have been also clarified as critical factors that affect the air infiltration. In this study, the indoor CO_2 concentration is detected and logged at three specific points in an office room for seven selected measurement-periods. The decay method is used to estimate the leakage rates. In parallel, an ultrasonic anemometer is used outdoors for monitoring wind characteristics, as the direction angle and the instantaneous velocity components, while the turbulence intensity is calculated. The results of ACH vary from $0,32h^{-1}$ to $0,75h^{-1}$ from measurement to measurement and thus an investigation is carried out from the perspective of unsteady windy conditions. A spectral analysis of the wind measurements is applied and the corresponding power spectra $S_{vv}(f)$ are correlated to the mean ACH of the room, giving a better understanding of wind-driven infiltration and depicting the role of the wind fluctuations frequency. In addition, a hypothesis of using the spatial distribution of CO_2 concentration indoors as airflow pattern tracer is presented respect to the location of the leakages and the local [CO_2] fluctuations are discussed as an indicator of leakage detection.

KEYWORDS

Wind-driven infiltration, Wind power spectral analysis, FFT, Turbulence intensity, Tracer gas, CO_2 decay method, Indoor building dynamics

1 INTRODUCTION

Air infiltration in buildings refers to the uncontrolled flow of outside air to the internal space through leakages in the envelope. Its impact on the energy consumption has been studied and clarified in a very early stage even (e.g. Caffrey, 1979; Persily, 1982; Anderlind, 1985). Air infiltration is caused either by wind-induced pressure differences across the building envelope or by the gradients between internal and external temperatures (Etheridge and Sandberg, 1996). Especially when the buoyancy forces are small, the wind-driven infiltration could potentially be the dominant mechanism (Shaw, 1981). The influence of climate characteristics, as the wind direction and the wind speed has been stated as factors that affect the air exchanges (Sherman, 1987).
Furthermore, the dynamic characteristics of air infiltration have been pointed (e.g. Hill and Kusuda, 1975) and therefore challenges arise upon that field. In particular, in low-rise

buildings the unsteady wind seems to govern the leakage rates (Brownell, 2002). Fluctuating wind causes unsteady flow phenomena that affect the instantaneous airflow rates across cracks and openings resulting to a deviation from the mean ones (e.g. Etheridge, 1999, Chaplin, 2000).
To estimate the infiltration rates of a building or a room, tracer gas techniques has been recognised as valuable and the their principles have been discussed (e.g. Sherman, 1990). In particular, carbon dioxide (CO_2) has been stated as a simple, cheap and proper gas to use for this purpose (Roulet, 2002). Recently, Labat *et al*. (Labat *et al.*, 2013) discussed the variation of the buildings air change rate (ACH) under natural conditions.
In this paper, CO_2 decay method is employed to estimate the mean leakage rates of a room and to correlate them to the wind direction and the wind velocity. In order to have a better understanding of wind-driven infiltration, a spectral analysis is performed providing additional information about the dynamic nature of wind and its impact on ACH. The results in the frequency-domain are presented and the role of the wind fluctuations frequency is discussed. Furthermore, the potential of using the indoors [CO_2] spatial distribution and the local [CO_2] fluctuations for leakages detection and as an airflow pattern tracer is asserted and linked to the outdoors wind conditions.

2 SETUP OF EXPERIMENT

2.1 Experimental field

The experimental work was carried out in the field of the meteorological station of the Norwegian University of Life Sciences (UMB) in Ås (59,66°N / 10,78°E). Figure 1a shows the field of the station and Figure 1b highlights the building in which the CO_2 measurement took place. The building is located at the south-west corner of the site. The orientation of the building deviates from the N-S axis by 6,5°. It consists of two compartments: an office room and a garage. The dimensions of each room as well as those of the whole building are shown in the Figure 2a.
The building is a typical Norwegian wooden construction of 70's (Fig. 2b). In particular, the garage is a non-heated space and consequently not insulated. Its external wall consists of only one layer (wooden cladding of 2*cm* thickness). In contrast, the office room is heated and insulated. The assembly of the external walls (~ 12,5*cm*) consists of five layers: wooden panel (1*cm*), vapor barrier, insulation (10*cm*), wind barrier and an external wooden cladding (1,5*cm*). The internal wall that separates the office from the garage is also insulated and wooden panels had been placed on both the interior and the 'exterior' surface (12*cm*). Finally, the ceiling is also insulated and its inner side consists of a wooden panel.
The measurements were carried out in the office room of the building. The dimensions of the net space of the room is 3,8*m* x 2,8*m* x 2,15*m* (V = 22,876m^3). The volume used hereinafter in the calculations refers to these dimensions. Figure 2c and 2d show the existence of a hole, in the north external wall of the building, in 2,1*m* height from the floor of the office room. The hole is circular (d_h = 2,5*cm*) and it services electrical issues as a cable (d_{cab} = 1*cm*) is fixed passing through. Based on the construction of the office room, it would be reasonable to claim that this hole constitutes a severe leakage path and probably the most important one. More precisely, the net area of the leakage-opening is ~ 4,12cm^2. In addition, the joints alongside the two windows of the room are taken into account as potential leakages. Finally, the door of the room was kept closed and sealed during the measurements.

Figure 1. (a) A satellite view of the experimental field and its surroundings. (b) The location of the building, at the SW corner of the experimental field.

2.2 Instruments

As mentioned above, the objective of this paper is to investigate the dynamic nature of air infiltration in buildings under unsteady wind conditions using CO_2 as tracer gas. In order to study the unsteady wind characteristics, an ultrasonic anemometer was used. Its principle is based on the transit time of ultrasonic acoustic signals. In particular, the following magnitudes were measured by the anemometer and logged in a PC: the three dimensional (3D) wind speed v, the three orthogonal velocities u, v and w, the wind direction angle θ_w, the wind elevation angle φ and the sonic-temperature of the ambient air.
The anemometer was placed on a mast at the same height as the hole-leakage (2,2m from the ground level) and in a distance of 11,5m from the north-oriented wall of the building (Fig. 1b). The sampling frequency was chosen as $f_w = 32Hz$, the fastest possible output rate given by the instrument, so that the dynamic wind characteristics would be detected. In order to be in harmony with other studies, the hourly 3D wind velocity on 10m from the main anemometer of the meteorological station was recorded as well.
For the purpose of measuring the infiltration rates of the office room, CO_2 detectors - loggers were used. In order to study the dynamics of the indoor, a frequency sampling of $f_g = 1Hz$ was chosen for logging the gas concentration. In total, three loggers were used, distributed at three different locations in the office room aiming to research the spatial variations of CO_2. The loggers were placed close to the hole-leakage (point A), close to the west-oriented window (point B) and the third one close to the sealed door (point C). All of them were on the same height that was defined as 0,8m. The logging points are noted in the Figure 2 by the red spots.
Finally, a pressurization test was applied in the office room, in order to get the air changes at 50Pa. The result showed that the $ACH_{50} = 8{,}17h^{-1}$, giving a general magnitude of the airtightness level. Consequently, following the relative 'rule-of-thumb', the annual infiltration rate of the room in operation is $n = 0{,}41h^{-1}$ (Sherman, 1998).

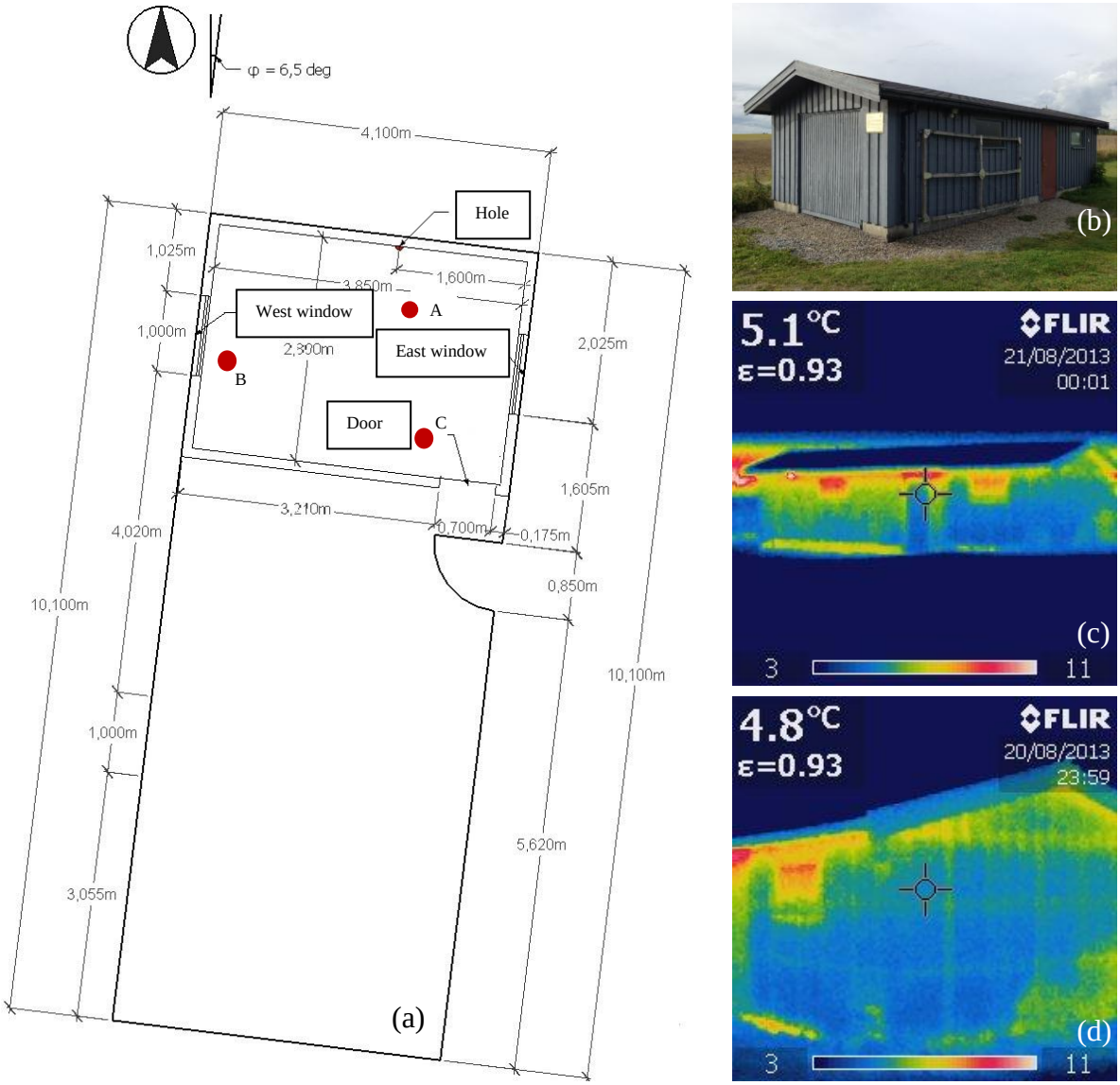

Figure 2. (a) Plan of the building, with the logging points A, B and C. The location of the hole across the north wall, the two windows and the door are shown as well. (b) The building is a typical Norwegian wooden construction of 70's. (c) Infrared picture of the building. (d) Infrared picture of the NE corner of the building.

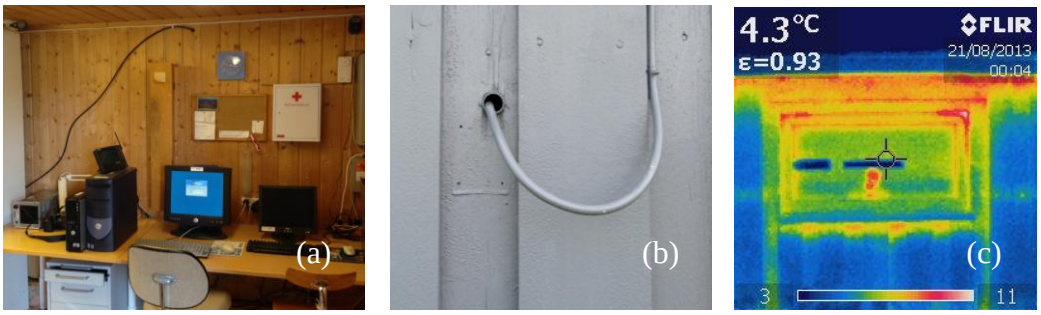

Figure 3. (a), (b) View of the leakage – hole, from inside and outside respectively. (c) Infrared picture of the leakages in the window that is west-oriented.

3 METHODOLOGY

The measurements were carried out during approximately periods of 3*h* on seven selected days and the annotation 'Day n' (n=1-7) is employed hereinafter. In order to have an overview of the wind conditions in each day, the Reynolds averaged wind velocity U was calculated as follows:

$$U = \overline{u^2 + v^2 + w^2} \tag{1}$$

where u, v and w are the three mean wind velocity components.
As mentioned above, the orientation of the building deviates from the N-S axis by only 6,5°. Thus, it is reasonable to claim that the longitudinal velocity component *v* in the axis N-S incidents by 90° angle on the north-oriented wall. In a similar way, we assume that the window close to the point B is west-oriented, while the other window east-oriented respectively.
The combined and synchronized use of an ultrasonic anemometer and CO_2 detectors with high sampling frequency provides the chance of investigating the dynamics of the wind-driven infiltration under unsteady conditions. Towards this scope, the calculation of the wind turbulence intensity I and the wind power spectrum, on each measurement day, seems to be helpful.
Wind turbulence can be generally described as fluctuations in the flow of air. The turbulence intensity is a scale characterizing turbulence as percent. In fact, it gives a picture of how large are the fluctuations of the wind flow compared to the mean value of the velocity. In other words, turbulence intensity *I* 'describes' the unsteadiness of wind and is calculated from the orthogonal velocity components *u*, *v* and *w* as follows:

$$I = \frac{\overline{\frac{1}{3}(u'^2 + v'^2 + w'^2)}}{\overline{u^2 + v^2 + w^2}} \tag{2}$$

where *u'*, *v'* and *w'* are the turbulent velocity fluctuations in E-W (lateral) axis, in N-S (longitudinal) axis and in the 'updraft' (normal) axis respectively. In the denominator, $U = \overline{u^2 + v^2 + w^2}$ is the Reynolds averaged velocity.
Furthermore, a spectral analysis is carried out in order to provide information about the wind energy distribution with respect to frequency. Thus, in this paper a Fast Fourier Transform (FFT) algorithm is applied into the fluctuations of the three orthogonal wind velocity components (here for the longitudinal velocity *v* in the N-S axis), in order to compute the Discrete Fourier Transform (DFT) and the frequency domain (Newland, 1975):

$$V'\ k\ = \sum_{n=0}^{N-1} v'\ n\ e^{-j2\pi nk/N} \tag{3}$$

where *V'*: the frequency domain representation of the wind fluctuations *v'* of the longitudinal velocity *v* in the axis N-S,
k: the kth frequency component,
n: the nth sample (in the time domain)
N: the total number of samples of *v*,
j: the imaginary unit.
Finally, the wind spectrum is calculated based on the following equation:

$$S_{vv}\ f\ =\ v'(f)\ ^2 = \int_{-\infty}^{\infty} v'(t)e^{-ift}dt \qquad (4)$$

In addition, the CO_2 'concentration test decay method' (ASTM – E741, 2006) is employed during the analysis of the data from the loggers placed indoors. In this way, the infiltration rates can be calculated in each case (day). The highest gas concentration that the loggers could detect and record was approximately 4000*ppm*. For each day, the initial and final times were determined and a normalized concentration C_N is calculated in each measurement time:

$$C_N = \ln \frac{C\ t\ - C_o}{C\ 0\ - C_o} \qquad (5)$$

where *C(t)*: the CO_2 concentration in the office room, as an average of the CO_2 concentrations detected in the three loggers,

C(0): the initial CO_2 concentration in the office room at t = 0*s*,

Co: the outdoors CO_2 concentration (it was about 410ppm).

Since the CO_2 concentration fluctuating as decaying, the 'average method' cannot be applied. Thus, in order to compute the ACH, the 'optional regression method' is used and a regression of ln*C(t)* needs to be performed according to (ASTM – E741, 2006):

$$\ln C_N = -At + \ln C_N(0) \qquad (6)$$

In the graphs of the C_N versus time a fitting line is added, the slope of which represents the mean infiltration rate ACH.

4 RESULTS AND DISCUSSION

4.1 ACH and wind characteristics

The normalized CO_2 concentration C_N for each measurement-day is computed and shown in the Figure 4. It is clear that the decay of the tracer gas is characterized by fluctuations. The necessary regression analysis is thus performed and the linear fitting line is presented in the Figure 4 along with the decay. As mentioned above, the slope of the fitting line is the mean ACH of the office room.

The values of the infiltration rates vary from 0,32h^{-1} to 0,75h^{-1}. The temperature gradients between outside and inside varies during the measurement-periods from 3$^{\circ}C$ to 7$^{\circ}C$, thus it would be reasonable to claim that the wind is the dominant mechanism of infiltration (Shaw, 1981). The lowest ACH took place on the day 1 and day 2 (ACH = 0,32 h^{-1}). During the measurement periods of those days the wind blows mainly from South (SSW-S on day 1 and SSE-S on day 2). The south-oriented side of the office room is wind-shielded, since it is the internal wall that separates the office from the garage. Given that the main leakages of the office are located on the east, west and north façade of the room, the relatively low ACH seem reasonable, despite of the large wind velocity (day 1: υ = 5,3*m/s* at 10*m* height and *U* = 3,7*m/s* at 2,2*m*, while for the day 2: υ = 5,0*m/s* at 10m and *U* = 3,4*m/s* at 2,2*m*).

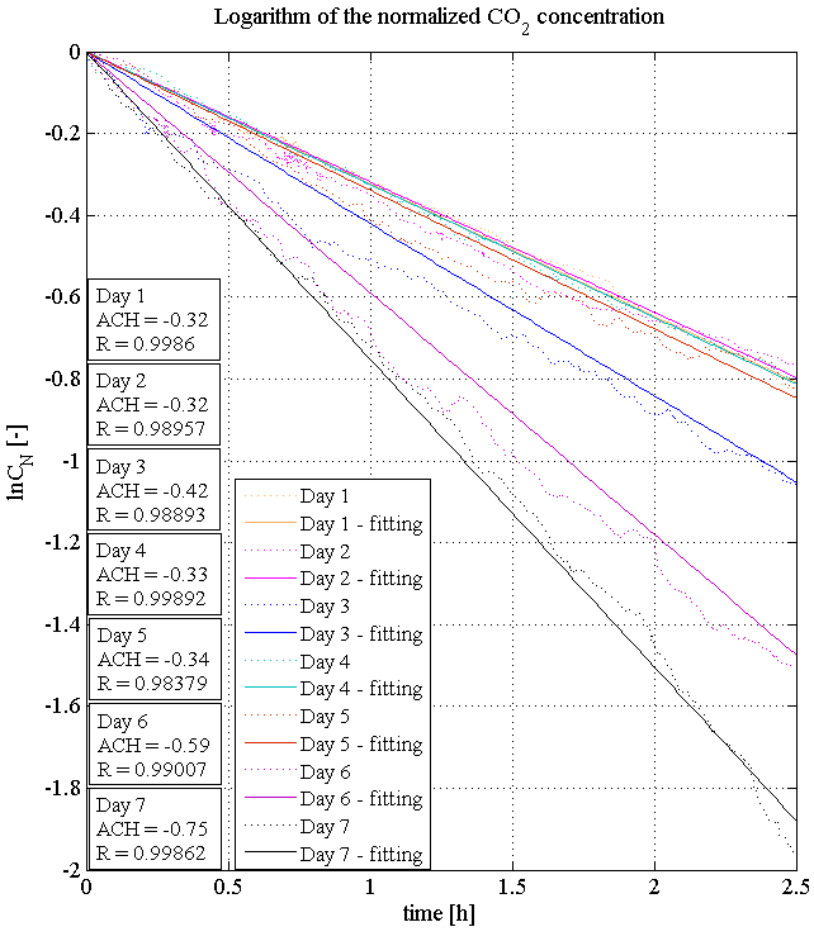

Figure 4. Logarithm of the average value of the CO_2 concentration in the three measurement locations versus the elapsed time since the start of decay.

During the days 3-7 the wind was blowing mainly from the North (or NNE and NE). A detailed overview of the wind direction angles during the measurements is provided in the Figure 5.

The higher infiltration rates during the days 3-7 can be explained by the fact that the north wall of the office room, where the hole is located, is in these cases exposed. Even though the wind direction is during those days fairly the same, the ACH vary from $0{,}33h^{-1}$ to $0{,}75\ h^{-1}$. The variations of the Reynolds averaged velocity U (or of 3D speed υ at 10m) can provide some arguments about these differences. Table 1 shows among other the 3D velocity υ at 10m, the Reynolds averaged velocity U at the height of the ultrasonic anemometer ($2{,}2m$) and the main wind direction angle θ_w. Since the main θ_w is in N-S axis, the respective wind velocity v was decided to be shown as well. In addition, the ACH rates for each measurement are summarized again and presented in Table 1 as well as the confidence intervals representing the dispersion of the [CO_2] around the fitting lines (using 99,9% confidence).

From the Table 1, it is clear that among the days 3-7 (that all correspond to the N or NE wind direction), the days 4 and 5 appear to have low ACH. Indeed, during these measurements the wind is milder compared to the other measurements. Thus, the impact of the wind velocity is getting justified as critical towards the estimation of building infiltration rates. In harmony with this, it is also the fact that during the day 7, when the highest velocity occurs ($\upsilon = 5{,}5m/s$ at $10m$ height and $U = 4m/s$ at $2{,}2m$), the ACH are the highest as well (ACH = $0{,}75\ h^{-1}$).

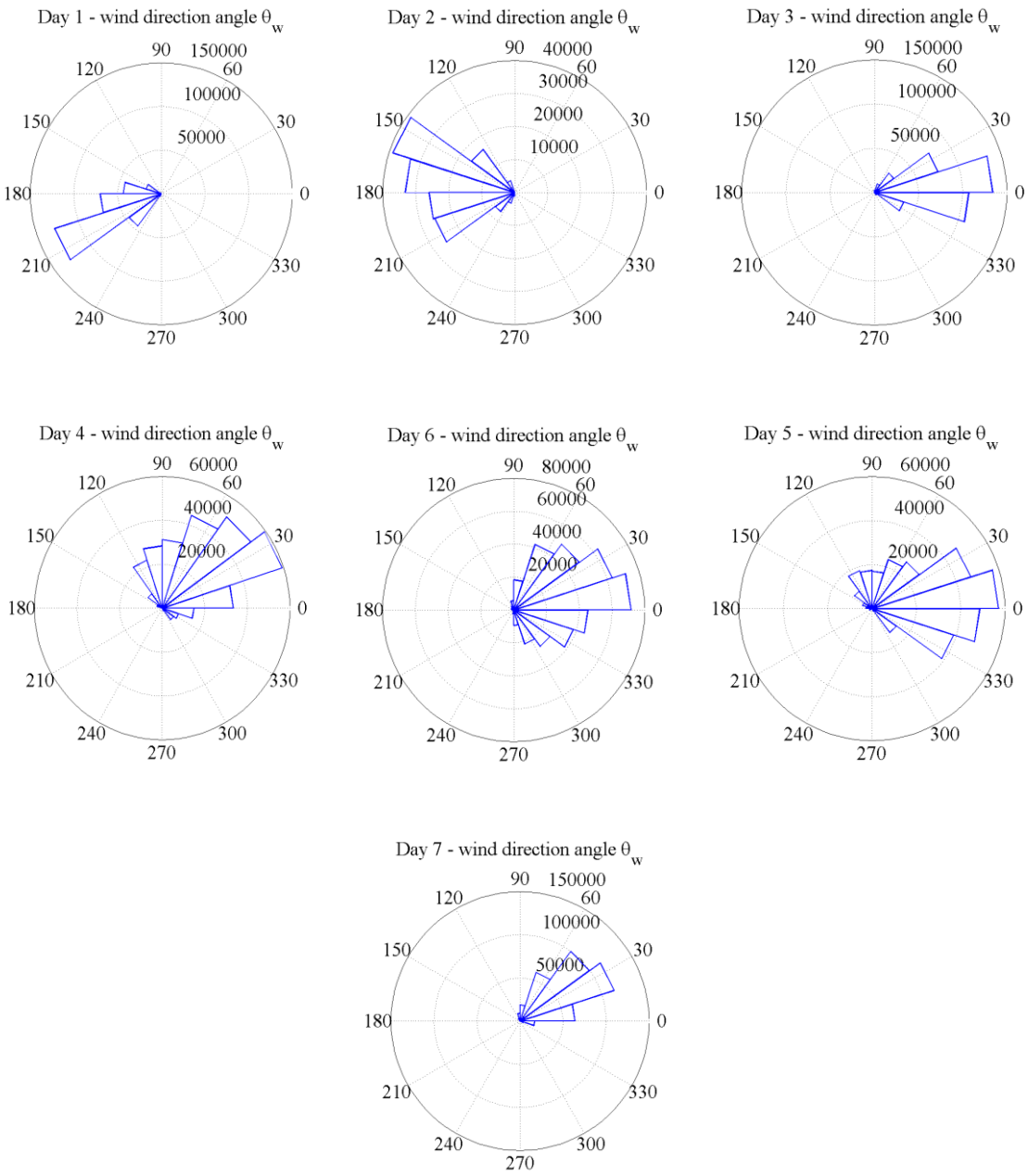

Figure 5. 'Windroses' depicting the variation of the wind direction angle θ_w during each measurement – day ($\theta_w = 0^\circ$ corresponds to North, $\theta_w = 90^\circ$ to East, $\theta_w = 180^\circ$ to South and $\theta_w = 270^\circ$ to West).

Table 1: Overview of the wind characteristics during the measurements and the respective ACH as calculated after a regression analysis applied.

	Wind speed *υ* (10m) [*m/s*]	**Reynolds averaged velocity *U* [*m/s*]**	**Wind velocity *v* in N-S axis [*m/s*]**	**Main wind angle θ_w [°]**	**Wind turbulence intensity I [%]**	**ACH [h^{-1}]**
Day 1	5,3	3,7	-3,2	SSW - S	28	0,32 ± 0,0004
Day 2	5,0	3,4	-3,0	SSE - S	36	0,32 ± 0,0012
Day 3	3,7	3,1	2,8	N	28	0,42 ± 0,0017
Day 4	3,4	2,5	1,2	NE	44	0,33 ± 0,0004
Day 5	2,9	2,1	1,5	N	47	0,34 ± 0,0016
Day 6	3,5	2,7	2,0	N - NNE	44	0,59 ± 0,0023
Day 7	5,5	4,0	2,9	NE	32	0,75 ± 0,0012

However, the results from the day 3 and 6 seem not to follow this 'rule'. In fact, even though the Reynolds averaged velocity *U*, as well as the longitudinal wind velocity component *v* in N-S axis, is higher in the day 3 than in the day 6, the ACH detected in the day 3 is lower than the respective in the day 6 ($ACH_3 = 0{,}42\ h^{-1}$, while $ACH_6 = 0{,}59\ h^{-1}$).
Thus, it would be reasonable to claim that neither the wind direction nor the wind velocity can fully play the role of safe criterion in order to determine the in-situ wind-driven infiltration. To research this 'disharmony' the turbulence intensity *I* (Table 1) and the wind power spectrum $S_{vv}(f)$ (Figure 6 and Figure 7) are computed, as has been described analytically in the methodology section. The turbulence intensity gives a magnitude of the amplitude of the fluctuations compared to the mean velocity. It can be extracted from the Table 1 that the intensity is not consistent with the results of ACH, thus no safe conclusion could be drawn.
In contrast to the intensity *I* (and the amplitude of the wind fluctuations) the wind power spectrum $S_{vv}(f)$ gives the energy distribution of the wind respect to the frequency of the fluctuations. The wind fluctuations frequency has already implied as critical parameter in a previous numerical study (Kraniotis *et al*., 2013). Since the wind angle is mainly North, the spectra of the longitudinal velocity *v* is decided to be presented.
As seen in Figure 6, even though the day 3 has slightly more energy than the day 6 in the very low frequencies (f~ <0,05*Hz*), the picture is opposite in higher frequencies. The spectrum of day 6 has more energy (two large peaks) than the respective of the day 3 in frequencies around $f = 0{,}15Hz$ ($0{,}1Hz < f < 0{,}2Hz$). Furthermore, the spectrum of day 6 seems also to include more energy than the day 3 in the high frequencies $0{,}5\ Hz < f < 1Hz$. In the very high frequencies, $f > 2Hz$, the two spectra appear to have similar picture.
Consistent with the previous research are the spectra of the other measurements as well. The day 7 seem to contain the higher energy among the measurement-days 3-7 in the frequencies f > 0,5Hz. Moreover, it appears to have by far higher energy than the other spectra in the very high frequencies f > 1Hz. The spectrum of the day 4 (that has the lowest ACH among the days 3-7) shows the highest energy in the very low frequencies (f ~ 0,03*Hz*), but it contains very little in the high frequencies (for $f < 0{,}7Hz$). The spectrum of the day 5, that it has also low ACH, seems to have fairly similar picture to the latter in the high frequencies. After all, it would be reasonable to claim that the high wind frequencies can play a determined role towards the evaluation of building ACH rates.

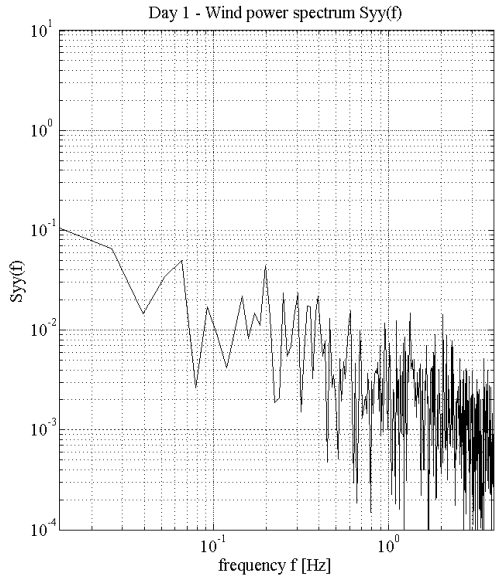

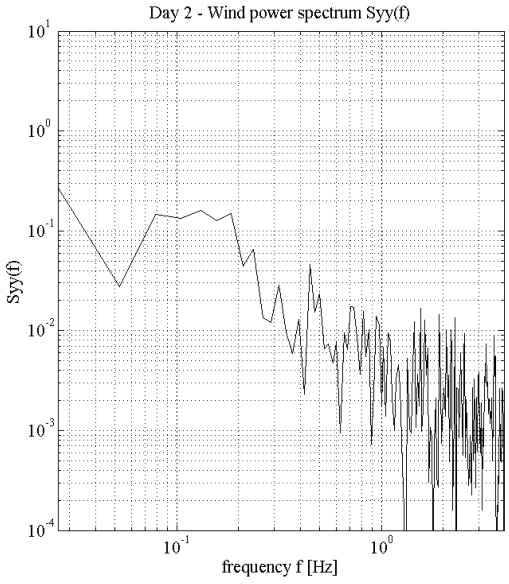

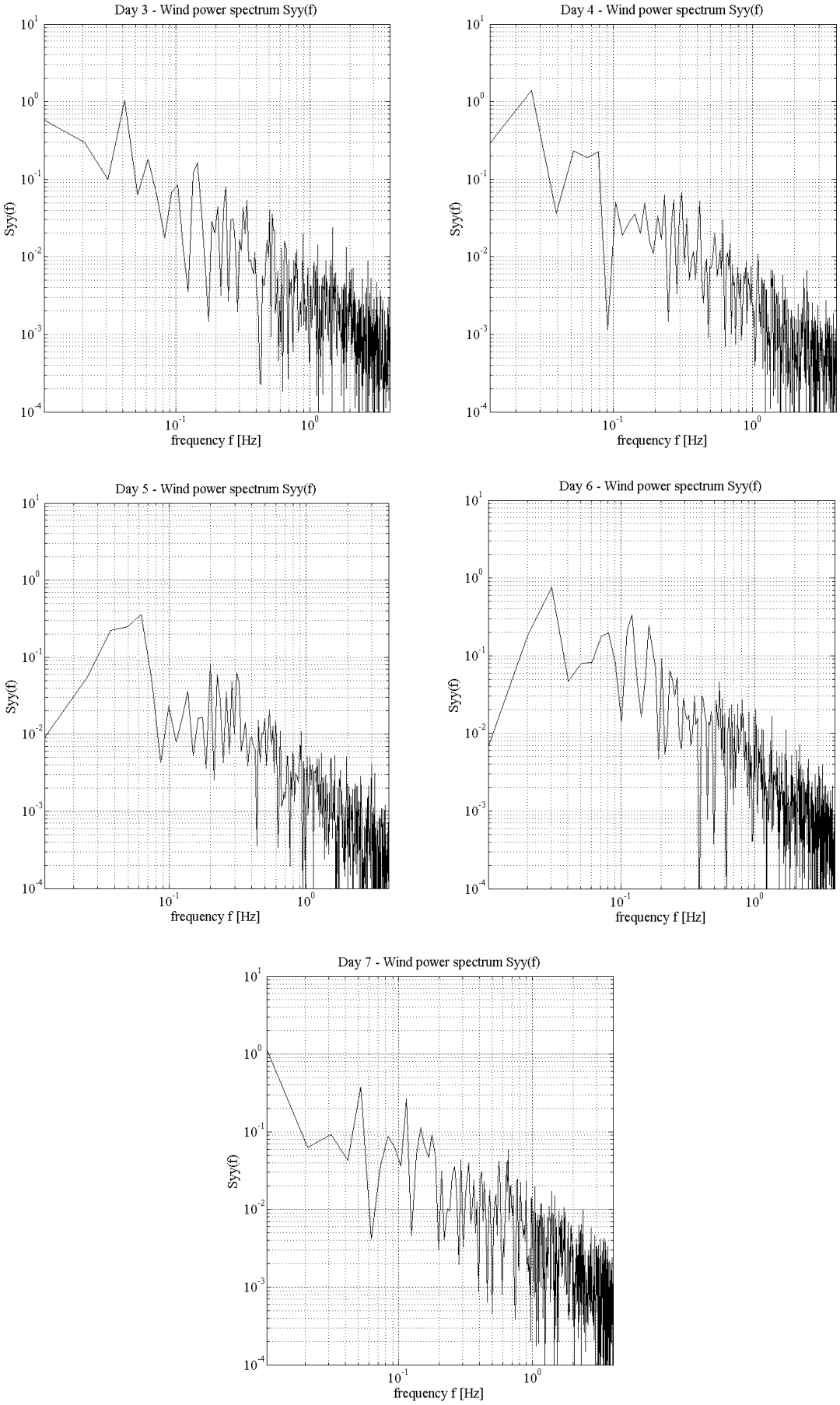

Figure 6. Wind power spectra of the longitudinal wind velocity *v* in the axis N-S.

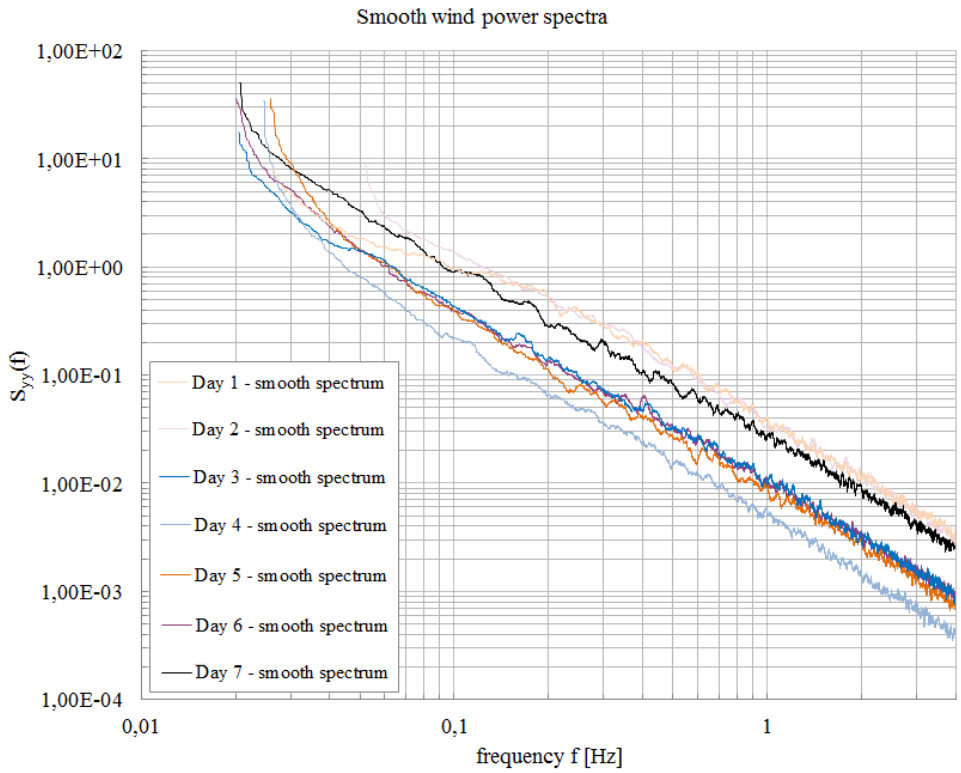

Figure 7. Smooth wind power spectra of the longitudinal wind velocity *v* in the axis N-S.

4.2 Spatial distribution of [CO_2]

Among the objectives of this paper is also the investigation of the spatial distribution of the CO2 concentration as well as its time variation. Detecting and logging the [CO_2] at multiple positions in the room may provide information regarding the indoor airflow patterns. The hypothesis is based on the fact that when the air enters the room is getting accelerated close the respective leakage (from it mainly enters), resulting in relatively higher ACH. In contrast, relatively lower ACH could imply a 'recession' of air flow, tending to a more 'stationary' regime. It should be noted that the logging-points A and C are located on an imaginary axis N-S, while the logging points B and C on an axis E-W. Figure 7 shows the ACH as calculated in each logging-point (A, B and C) after the regression analysis applied.

For the measurement-day 1, when the wind direction is SSW-S, it happens that $ACH_C = ACH_B > ACH_A$. Following the hypothesis stated above, the air flows from the axis C - B $\rightarrow$ A. Indeed, respect to the wind direction, it would be reasonable to claim that the air may enters from the west-oriented window, which is very close located to the logging-point C and then it follows the 'axis' C – B. It finally results into the point A, which is north-oriented and consequently well-shielded from a SSW-S wind.

For the measurement-day 2, $ACH_B > ACH_C > ACH_A$. In this case the wind direction is SSE-S, it could be assumed that the air mainly flows into the room from the east-oriented window (close to logging point B) and following the 'axis' B – C, results into the leakage A.

All the measurement-days 3-7 (apart from the day 3) seem to respect the hypothesis as well respect to the corresponding wind direction. In all those cases it happens that $ACH_A > ACH_C > ACH_B$, implying that the air enters from the leakage A and respecting the mainly North wind, flows on the 'axis' A – C, which is parallel to N-S, and then is getting dissipated and 'stationary' at the point B.

Finally, table 2 shows the standard deviation σ of the ACH at each logging-point for all the measurement-periods. The values imply the 'fluctuations' of the [CO_2] at the certain point. It seems that for the point C the σ is higher compared to the points A and B, for all the cases. Given that the point C is close to the sealed door, it would be reasonable to claim that the [CO_2] fluctuates because of the wall boundary conditions on the that side of the office room. Again, the relatively small leakage area of the point C most likely 'blocks' the flow when it is normal (90° angle) to it, resulting in oscillations of the [CO_2]. In contrast a logger close to a relatively bigger leakage area may detects less [CO_2] fluctuations, as the air could exfiltrate or infiltrate more easily and the flow is more 'smooth', implying boundary conditions more similar to an 'opening'.

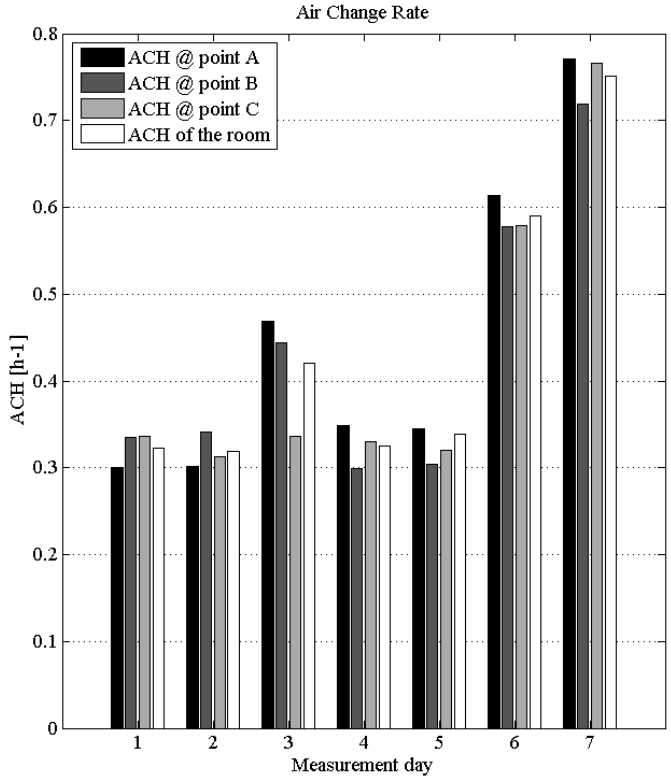

Figure 7. Air change rates (after the regression analysis) at each logging-point for each measurement-day.

Table 2: Standard deviation σ of the ACH at the three logging-points.

	Day 1	**Day 2**	**Day 3**	**Day 4**	**Day 5**	**Day 6**	**Day 7**
σ of point A	0,0139	0,0405	0,0705	0,0182	0,0534	0,0795	0,0410
σ of point B	0,0102	0,0387	0,0726	0,0160	0,0371	0,0998	0,0407
σ of point C	0,0304	0,0481	0,0834	0,0392	0,0675	0,1008	0,0607

5 CONCLUSIONS

The indoor CO_2 concentration ([CO_2]) is detected and logged at three specific points in the office room of the meteorological station of the Norwegian University of Life Sciences

(UMB). In parallel, an ultrasonic anemometer is used outdoors for monitoring wind characteristics, as the direction angle and the instantaneous velocity components. In total seven measurement-periods are presented in this paper.
The CO_2 decay method is employed to calculate the infiltration rates of the room in each measurement (day 1-7), using a regression analysis. The results show that ACH vary from $0{,}32h^{-1}$ to $0{,}75h^{-1}$. The south wall of the room is wind-shielded and the lowest values take place when the wind is South, justifying the influence of wind direction angle. However, the ACH show large differences even among the measurement-days that the main wind direction is the same (North wind). A study on the wind speed, the Reynolds average wind velocity and the longitudinal velocity component provides some arguments for the variation of the leakage rates. Nevertheless, the mean values of the wind velocity are not enough to explain the whole picture of ACH variation. Therefore, the turbulence intensity is calculated and a spectral analysis is performed in order to investigate the dynamic characteristics of the unsteady wind. The amplitude of wind fluctuations (turbulence intensity) cannot be straightforward correlated to the ACH, while their frequency characteristics (wind power spectra) provide a better understanding of wind-driven infiltration, implying the role that high wind fluctuations frequency and the potential to cause higher ACH.
Finally, a hypothesis of using the spatial distribution of $[CO_2]$ indoors as airflow pattern tracer is presented respect to the location of the leakages. It seems low $[CO_2]$ levels (and consequently high ACH) characterise positions close to where air flows into the room, while higher values of $[CO_2]$ (and consequently low ACH) take place at positions that the flow is getting recessed, described by a more 'stationary' regime. In addition, the fluctuations of the indoors $[CO_2]$ seem that potentially could be an indicator of the boundary conditions of the respective position. When the airflow is normal (90° angle) to relatively small leakage areas is reasonable to claim that is getting 'blocked' ('wall' boundary conditions), resulting in a locally oscillating phenomenon. In contrast, an area close to a relatively big leakage path is more likely characterized by a 'smooth' flow, when the angle is 90°, and thus the local $[CO_2]$ fluctuations may be relatively small, implying 'opening-type boundary conditions.
The paper sets up issues regarding the impact of the unsteady wind on the air exchanges. Maybe a more detailed study of the dynamic wind characteristics through a spectral analysis ought to provide a more detailed view of the wind-driven infiltration, especially in cases that the latter is more important mechanism than the buoyancy forces. Further research need to be done in order to enhance the results regarding the role of the wind fluctuations frequency and to investigate the local building dynamic phenomena with respect to the leakage magnitude and distribution.

6 REFERENCES

Anderlind, G. (1985). *Energy consumption due to air infiltration*. Proceedings of the 3rd ASHRAE/DOE/BTECC Conference on Thermal Performance of Exterior Envelopes of Buildings, Clear Water Beach, FL, 201–208.

ASTM International (2006). *Standard test method for determining air change in a single zone by means of a tracer gas dilution*.

Brownell, C., 2002. *Infiltration heat recovery*. Duke University, Durham, NC.

Caffey, G.E. (1979). *Residential air infiltration*. ASHRAE Transactions (85), 919–926.

Chaplin, G.C., Randall, J.R., Baker C.J. (2000). *The turbulent ventilation of a single opening enclosure*. Journal of Wind Engineering and Industrial Aerodynamics (85), 145–161.

Etheridge, D.W., Sandberg, M. (1996). *Building ventilation: Theory and measurement*. Wiley.

Etheridge, D.W. (1999). *Unsteady wind effects in natural ventilation design*. CIBSE National Conference, Harrogate

Hill, J.E., Kusuda, T., 1975. *Dynamic characteristics of air infiltration*. ASHRAE Transactions. (81)1, 168–185.

Kraniotis, D., Thiis, T.K., Aurlien, T. (2013). Wind direction and leakage distribution. A CFD transient analysis of their impact on air exchange rates under unsteady wind conditions. 6th European – African Conference on Wind Engineering, Cambridge, UK.

Labat, M., Woloszyn, M., Garnier, G., Roux, J.J. (2013). *Assessment of the air change rate of airtight buildings under natural conditions using the tracer gas technique. Comparison with numerical modelling.* Building and Environment (60) 37–44.

Newland, D.E. (1975). An introduction to random vibrations, spectral and wavelet analysis. Longman Scientific & Technical.

Persily, A. (1982). *Understanding air infiltration in homes*. Report PU/CEES No. 129. Princeton University Center for Energy and Environmental Studies, Princeton, NJ.

Roulet, C.A., Foradini, F. (2002). Simple and cheap air change rate measurement using CO_2 concentration decays. International Journal of Ventilation (1), 39–44.

Shaw, C.-Y. (1981). *A correlation between air infiltration and air tightness for houses in a developed residential area*, National Research Council Canada, Ottawa.

Sherman M.H. (1987). *Estimation of infiltration from leakages and climate indicators*. Energy and buildings (10), 81–86.

Sherman M.H. (1990). *Tracer-gas techniques for measuring ventilation in a single zone*. Building and Environment (25) 4, 365–374.

Sherman, M.H. (1998). *The use of blower-door data*, Lawrence Berkeley National Laboratory.